







C and L band fiber lasers enhanced by ultrafast laser inscribed artificial backscatter reflectors

ROSA ANA PEREZ-HERRERA,^{1,2,*}  P. ROLDAN-VARONA,^{3,4,5} 
A. SANCHEZ-GONZALEZ,^{1,2} L. RODRIGUEZ COBO,⁴
J. M. LOPEZ-HIGUERA,^{3,4,5}  AND M. LOPEZ-AMO^{1,2} 

¹Department of Electrical, Electronic and Communication Engineering, Public University of Navarra, 31006 Pamplona, Spain

²Institute of Smart Cities (ISC), Public University of Navarra, 31006 Pamplona, Spain

³Photonics Engineering Group, University of Cantabria, 39005 Santander, Spain

⁴CIBER-bbn, Instituto de Salud Carlos III, 28029 Madrid, Spain

⁵Instituto de Investigacion Sanitaria Valdecilla (IDIVAL), 39005 Cantabria, Spain

*rosa.perez@unavarra.es

Abstract: This letter presents an experimental comparison between two linear-cavity erbium-doped fiber lasers (EDFL) assisted by two different artificial backscatter fiber-based reflectors. Both reflectors were inscribed by femtosecond laser direct writing, one of them within a single-mode fiber (SMF) and the other one within a multi-mode fiber (MMF). Although the erbium-doped fiber amplifier (EDFA) used in both structures was the same and both reflectors were manufactured under the same parameters, the reflection spectrum of each was clearly different due to their different physical properties. The first linear-cavity EDFL, consisting of an SMF-based reflector with 9 μ m core and 125 μ m cladding, resulted in a single laser emission line located in the C-band and centered at 1564.4 nm, exhibiting an optical signal-to-noise ratio (OSNR) of 52dB when pumped at 100mW. On the other hand, a single laser emission line with a similar OSNR but in L-band (centered at 1574.5nm) was obtained when using an MMF-based reflector with 50 μ m core and 125 μ m cladding.

© 2022 Optica Publishing Group under the terms of the [Optica Open Access Publishing Agreement](#)

1. Introduction

Femtosecond (fs) laser direct-write optical fiber structures have proven to be of great interest for a wide range of applications [1]. Fundamentally, the permanent changes induced by the tight focusing of fs laser pulses can be divided into three major groups: smooth isotropic refractive index change (RIC), birefringent RIC, or empty hole (ablation) [2], [3]. This inscription technique allows the fabrication of microstructures in diverse types of transparent optical materials, such as multicore optical fibers [4], fluoride glass [5], few-mode optical fibers (FMF) [6], no-core fibers (NCF) [7], or polymer optical fibers (POF) [8], among others. Fs laser direct-write technology can be used to fabricate different fiber-optic interferometer structures, such as Fabry-Perot interferometers (FPIs), [9], Mach-Zehnder interferometers (MZIs) [1], [10], or Michelson interferometers (MIs) [11]. It is well known that it is not possible to inscribe gratings in non-photosensitive fibers by means of UV phase mask technique. However, fs laser writing allows to inscribe structures such as fiber Bragg gratings (FBG) [12], [13], long period fiber gratings (LPGs) [14–16], tilted fiber Bragg gratings (TFBGs) [17] or random fiber gratings (RFG) [18], [19], among others [20]. These RICs result in optical fiber structures that, like a grating, behave like artificially controlled backscatter (ACB) fiber reflectors than can be inserted into a linear cavity fiber-optic laser.

Periodical or random, distributed or quasi-distributed grating-based ACB reflectors have been also used to obtain tunable, switchable, or multiwavelength laser outputs [18], [19]. These distributed reflective microstructures exhibit similar temperature sensitivity to traditional uniform

FBGs. However, it has been demonstrated that the random periodicity in these RICs can result in sensitivities to strain variations of up to an order of magnitude higher [21].

Recently published studies have shown that such distributed reflectors, fabricated by fs inscription on SMF, can produce narrow lasers with OSNR values up to 60 dB [22]. However, these inscriptions had to be up to 10 cm long, and their application has been demonstrated only at the C-band. In the present work, we show how this technique can be extended to the L-band using only MMF fiber and reaching comparable OSNR values in both emission bands and with reflectors as compact as 17 mm in length.

Here, a comparison between two linear-cavity EDFLs, assisted by two different artificial backscatter reflectors, both inscribed by means of an fs laser, is experimentally carried out. The same inscription parameters were used for both types of artificial backscatter fiber-based reflectors, and both were inscribed along the central axis of the fiber core with a length as short as 17 mm each. The only difference between them was the dimensions of the fiber employed, being the first artificial backscatter reflector fabricated within a standard single-mode fiber (SMF-ABR) with 9 μm core and 125 μm cladding, and the second one within a multi-mode fiber (MMF-ABR) with 50 μm core and 125 μm cladding. The linear-cavity EDFL including the SMF-based reflector resulted in a single laser emission line located in the C-band, while a single laser emission line but in L-band was measured when using the MMF-based reflector.

2. Inscription process

All ultrafast laser writing was performed using a Cazadero fiber laser (Calmar Laser) that delivers 370 fs laser pulses at a central wavelength of 1030 nm. However, the light absorbed non-linearly by the fiber has a wavelength of 515 nm, due to the second harmonic generation (SHG) introduced in the setup, as shown in [23]. A pulse repetition rate of 150 Hz and a pulse energy of 0.75 μJ were used. The laser pulses were tightly focused into the $\text{\O}50 \mu\text{m}$ core of a multimode fiber (MMF) using a 0.42 NA, 50 \times objective lens from Mitutoyo. The fiber was translated through the laser focus using a motorized nano-resolution XYZ stage from Aerotech.

Both SMF and MMF artificial backscatter reflectors have a length of only 17 mm, and a random period between $\Lambda_{\min} = 1.61085 \mu\text{m}$ and $\Lambda_{\max} = 1.64230 \mu\text{m}$. The optical structures are written on the axial axis of the fiber. In these ACB reflectors [19], the almost total periodicity of the optical structure gives rise to Bragg resonances which, in the third order ($m = 3$), present reflections in the following spectral bands:

$$\lambda_B = \frac{2}{m} n_{\text{eff}} \Lambda = \begin{cases} \text{SMF} \rightarrow n_{\text{eff}} \approx 1.4427; \lambda_B \approx 1564.4 \text{ nm} \\ \text{MMF} \rightarrow n_{\text{eff}} \approx 1.4528; \lambda_B \approx 1575.4 \text{ nm} \end{cases} \quad (1)$$

where Λ refers to the period of the structure (it is assumed $\Lambda = (\Lambda_{\min} + \Lambda_{\max})/2$), m is the order of resonance, n_{eff} is the effective refractive index, and λ_B is the Bragg wavelength.

3. Characterization process

Both artificial backscatter fiber-based reflectors were characterized by means of an ultra-high spatial resolution optical backscattered reflectometer (OBR 4600, from LUNA), used for fiber testing [24]. To avoid undesired reflections, free terminations of the fiber-based reflectors were immersed into index-matching oil.

As mentioned above, these two reflectors were manufactured using the same inscription parameters and located along the axial axis of the fiber. However, as it will be seen in the following figures, frequency and time domain responses of these two fiber-based reflectors will differ significantly. To help identify the results, the measurements obtained when using the SMF-ABR are depicted in black, while the measurements when using the MMF-RFG are shown in blue.

Figures 1(a) and 1(b) show the backscattered optical power as a function of the fiber length for the SMF-ABR and the MMF-ABR, in that order. These measurements were performed in the time-domain acquisition mode achieving a spatial resolution of 0.1 mm and the length of both inscriptions was 17 mm. These two fiber samples were located approximately 2.78 m and 2.84 m from the connector of the OBR, as illustrated in Figs. 1(a) and 1(b) respectively. Each one of these fiber-based reflectors presents different amplitudes of backscattered light along the length of the fiber due to refractive index fluctuations [19].

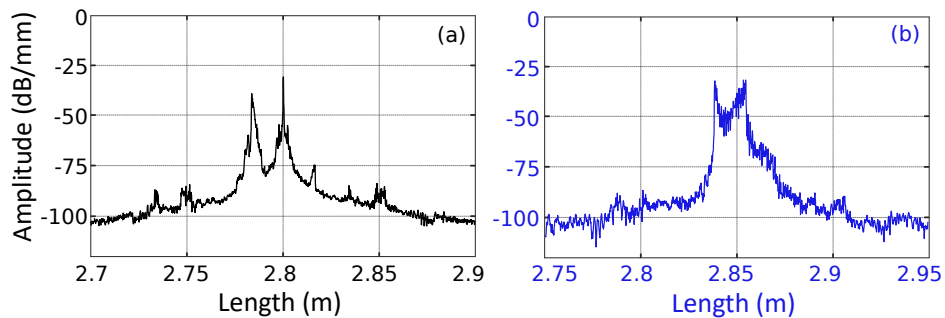


Fig. 1. Reflectogram of the (a) SMF-ABR or (b) MMF-ABR, measured by the OBR in the time-domain acquisition mode.

As shown in Fig. 1(a) and Fig. 1(b), an amplitude up to 50 dB over the noise floor at the beginning and end of SMF and MMF artificial backscatter reflectors were measured, varying this value along the center of the reflector depending on the type of fiber on which it was inscribed.

Figures 2(a) and 2(b) present the reflectance spectra as a function of wavelength for the artificial backscatter reflector fabricated into an SMF or an MMF, respectively. These measurements were carried out in the frequency-domain acquisition mode with a resolution bandwidth of 0.1 GHz over a wavelength range from 1545.52 nm to 1588.26 nm. These spectra show a non-flat response, with maximum values of around -10 dB at 1564.4 nm and 1575.4 nm for the SMF and MMF-based reflector respectively. These maximum values agree with the obtained results shown in Eq. (1) and will assist in forcing the laser emission around those wavelengths. Moreover, it can be observed that the non-flat response of the MMF-ABR presents a random ripple of up to 20 dB in amplitude, more than four times higher than the case of the SMF-ABR. This was to be expected given the multimodal nature of the MMF-ABR, resulting in a noisier response when compared to the SMF-ABR.

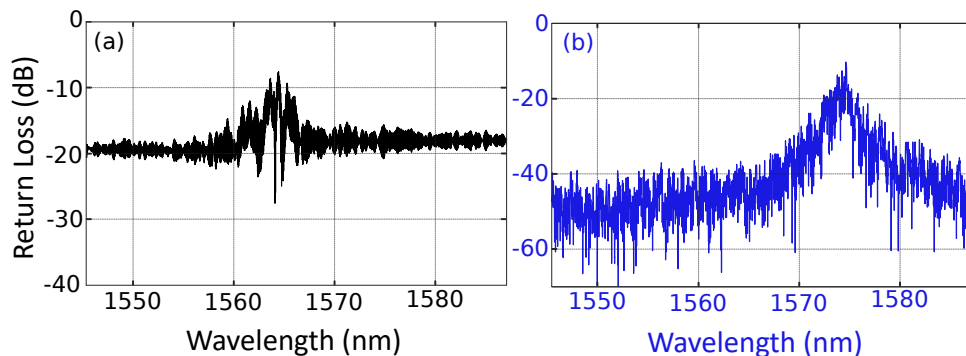


Fig. 2. Reflectance spectrum of the (a) SMF-ABR or (b) MMF-ABR as a function of the wavelength, measured by the OBR in the frequency-domain acquisition mode.

4. Experimental setup

The schematic diagram of the linear-cavity EDFL experimental setup, in which an artificial backscatter reflector inscribed into an SMF or into an MMF was used as distributed mirror, is depicted in Fig. 3. As illustrated, a 980/1550 nm wavelength division multiplexer (WDM) was used to inject the 976 nm pump power into the linear-cavity EDFL. The gain medium was placed at one of its ends and connected to the common port of the WDM. It consisted on 5 meters of highly Er-doped fiber (EDF) followed by a 3-ports optical circulator in which ports 3 and 1 were connected to conform a fiber loop mirror (FLM), as in [25].

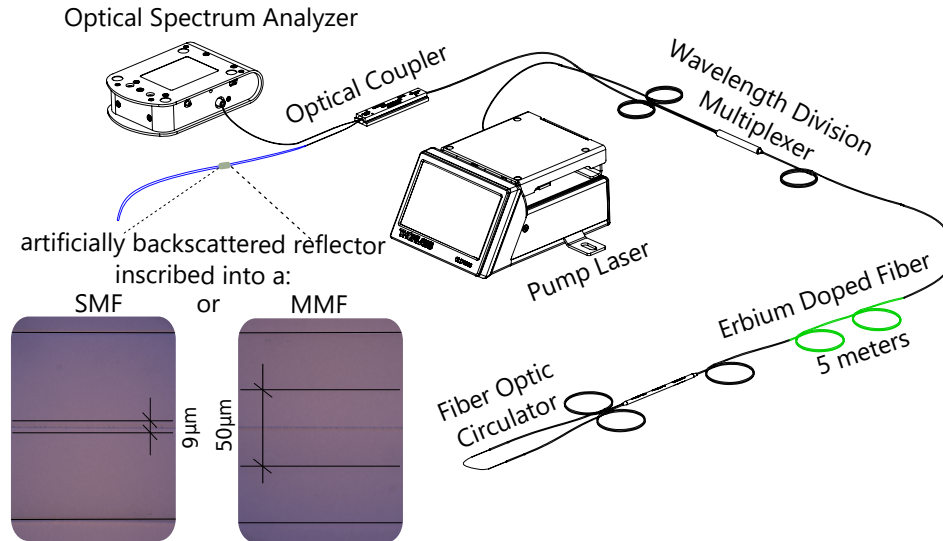


Fig. 3. Schematic diagram of the experimental linear-cavity EDFL setup, in which an artificial backscatter reflector inscribed into an SMF or into an MMF were used as reflectors.

The gain medium used was the I-25 (980/125) (Fibercore Inc.), suitable for C-band amplifiers with a core composition optimized for EDF amplifiers (EDFAs) in dense-WDM (DWDM) networks and a peak core absorption ranges from 7.7 to 9.4 dB/m at 1531 nm [25]. The reflected signal from the FLM passed through the highly EDF section again and it reached the 1550 nm-port of the WDM up to an optical coupler. At this point, the signal is divided into two branches where 90% of the signal reached the artificial backscatter fiber reflector, which can be inscribed into an SMF or an MMF (as can be seen in the two pictures inside the figure). The remaining 10% of the signal was monitored with an optical spectrum analyzer (OSA) with a resolution of 30 pm and a sensitivity of -75 dBm.

As in previous studies, both free ends of the artificial backscatter fiber-based reflectors were immersed in refractive index-matching oil to avoid undesired reflections. All the experimental measurements were carried out at room temperature, and no vibration isolation or temperature compensation techniques were employed.

5. Results and discussion

The output spectra of these linear-cavity EDFLs when pumped by a 976 nm source at 100 mW are presented in Figs. 4(a) and 4(b). As expected, and considering the above results, in both cases single-wavelength lasers with output power levels of -8.41 dBm and -7.18 dBm were obtained when using an SMF-ABR (Fig. 4(a)) and an MMF-ABR (Fig. 4(b)), respectively. This constitutes a significant improvement over previous results using quasi-distributed grating-based

ACB reflectors [26]. In addition, the configuration with an SMF-ABR presented an optical signal-to-noise ratio (OSNR) of 50.57 dB, markedly lower than the 57.31 dB obtained in the case of MMF-ABR. This was, however, to be expected when considering the different extinction ratios obtained for both reflectors, as shown in Fig. 2. It is worth noting that in both cases an OSNR greater than 50 dB was achieved, demonstrated to be reasonably good for most sensor applications [21], [27].

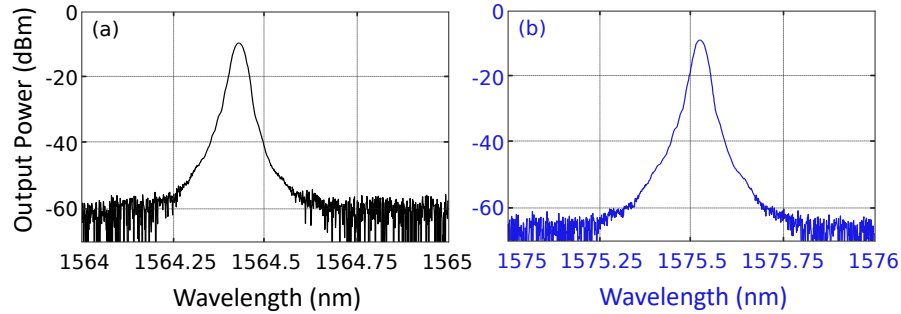


Fig. 4. Output spectra of the linear-cavity EDFL, pumped by a 976-nm light at 100 mW when using (a) an SMF-ABR or (b) an MMF-ABR.

After that, the output port previously monitored by an OSA was connected to a photodetector in combination with an electrical spectrum analyzer (ESA) to perform the characterization in the electrical frequency domain. Heterodyne detection of these two linear-cavities was carried out by using a 3dB optical coupler for mixing their signal with a tunable laser source (TLS) whose FWHM linewidth was 100 kHz [18]. Figures 5(a) and 5(b) illustrate the experimental characterization of the longitudinal-mode behavior when using an artificial backscatter reflector inscribed into an SMF or into an MMF, respectively. The measured frequency spectra corresponding to the frequency domain conversion clearly show the appearance of multiple longitudinal mode beating so, both present a multimode operation.

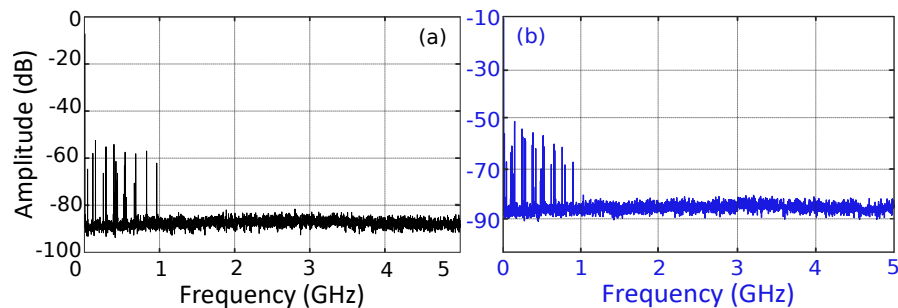


Fig. 5. Radio-frequency spectra of the linear-cavity EDFL beaten with the TLS when using (a) an SMF-ABR or (b) an MMF-ABR.

To evaluate the output spectra of the laser, the linear-cavity EDFL was pumped with powers ranging from 0 to 300 mW. Figures 6(a) and 6(b) depict the relationship between the output power levels as a function of the 976 nm pump power for the SMF-ABR or the MMF-ABR-based fiber lasers, respectively. These two figures show very similar results in terms of both threshold pump power and laser efficiency. When an SMF-ABR was used as a distributed reflector, a threshold pump power of 50 mW and an optical efficiency of 0.24% were achieved. Similarly, a threshold pump power of 53 mW and an optical efficiency of 0.25% were measured when an MMF-ABR

was employed as a reflector. These configurations also show a considerable reduction of the required length of feedback SMF when compared to similar works [28]. In these earlier studies, hundreds of meters of ACB-SMF were needed to obtain similar threshold pump power values and even lower OSNR levels than those presented here.

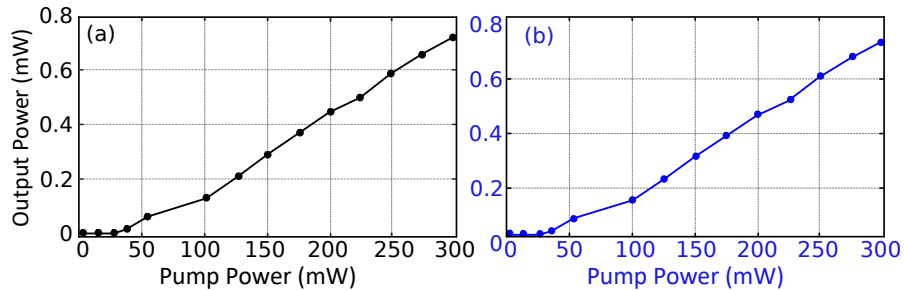


Fig. 6. Relationship between the output power levels versus 976-nm pump power for (a) the SMF-ABR-based fiber laser or (b) the MMF-ABR-based fiber laser.

6. Conclusions

In this letter, an experimental comparison between two linear-cavity erbium-doped fiber lasers assisted by artificial backscatter reflectors is presented. All the inscription parameters used to fabricate these two types compact artificially controlled backscattering fiber reflectors were the same. Both of them were inscribed along only 17 mm of the central axis of the fiber core. However, the first one was fabricated within a 9/125 SMF and the second one within a 50/125 MMF. When these fiber-based reflectors were inserted into a linear-cavity EDFL, the obtained reflection spectra of each was noticeably different. The linear-cavity EDFL including the SMF-based reflector resulted in a single laser emission line located in the C-band and centered at 1564.4 nm. On the other hand, a single laser emission line but in L-band and centered at 1574.5 nm was obtained when using the MMF-based reflector. Both cases presented similar OSNRs of 52 dB when pumped at 100 mW. This demonstrates, for the first time to the authors' knowledge, the ability of these structures to implement all-fiber lasers not only at C-band but also at L-band using only standard fibers.

Funding. Ministerio de Educación, Cultura y Deporte (PhD grant FPU2018/02797); European Commission (Next generation EU/PTR); FEDER (A way to make Europe); MCIN/AEI/10.13039/501100011033 (PDC2021-121172-C21, PID2019-107270RB).

Disclosures. The authors declare no conflicts of interest.

Data availability. Data underlying the results presented in this paper are not publicly available at this time but may be obtained from the authors upon reasonable request.

References

1. J. Zhao, Y. Zhao, Y. Peng, R. Lv, and Q. Zhao, "Review of femtosecond laser direct writing fiber-optic structures based on refractive index modification and their applications," *Opt. Laser Technol.* **146**, 107473 (2022).
2. R. Gattass and E. Mazur, "Femtosecond laser micromachining in transparent materials," *Nat. Photonics* **2**(4), 219–225 (2008).
3. S.M. Eaton, G. Cerullo, and R. Osellame, "Fundamentals of femtosecond laser modification of bulk dielectrics in Femtosecond Laser Micromachining," R. Osellame, G. Cerullo, and R. Ramponi, eds. 3–18 (Springer, 2012).
4. C. Zhang, Z. Jiang, S. Fu, M. Tang, W. Tong, and D. Liu, "Femtosecond laser enabled selective micro-holes drilling on the multicore-fiber facet for displacement sensor application," *Opt. Express* **27**(8), 10777 (2019).
5. J.-P. Bérubé, M. Bernier, and R. Vallée, "Femtosecond laser-induced refractive index modifications in fluoride glass," *Opt. Mater. Express* **3**(5), 598 (2013).
6. C. Yang, C. Zhang, S. Fu, L. Shen, Y. Wang, and Y. Qin, "Mode converter with C + L band coverage based on the femtosecond laser inscribed long period fiber grating," *Opt. Lett.* **46**(14), 3340 (2021).

7. Q. Wang, H. Zhang, and D. N. Wang, "Cascaded multiple Fabry–Perot interferometers fabricated in no-core fiber with a waveguide for high-temperature sensing," *Opt. Lett.* **44**(21), 5145 (2019).
8. G. Woyessa, A. Theodosiou, C. Markos, K. Kalli, and O. Bang, "Single Peak Fiber Bragg Grating Sensors in Tapered Multimode Polymer Optical Fibers," *J. Light. Technol.* **39**(21), 6934–6941 (2021).
9. Y. Liu and S. L. Qu, "Optical fiber Fabry-Perot interferometer cavity fabricated by femtosecond laser-induced water breakdown for refractive index sensing," *Appl. Opt.* **53**(3), 469 (2014).
10. Y. Liu, G. Q. Wu, R. X. Gao, and S. L. Qu, "High-quality Mach-Zehnder interferometer based on a microcavity in single-multi-single mode fiber structure for refractive index sensing," *Appl. Opt.* **56**(4), 847 (2017).
11. Y. Liu and D. N. Wang, "Fiber In-Line Michelson Interferometer Based on Inclined Narrow Slit Crossing the Fiber Core," *IEEE Photonics Technol. Lett.* **30**(3), 293–296 (2018).
12. X. Dong, L. Zeng, D. Chu, and X. Sun, "Highly Sensitive Dual Parameter Sensor Based on a Hybrid Structure with Multimode Interferometer and Fiber Bragg Grating Fabricated by Femtosecond Laser," *Sensors* **21**(17), 5938 (2021).
13. W. Bao, S. Liu, W. Feng, and Y. Wang, "Fiber Bragg Grating with Enhanced Cladding Modes Inscribed by Femtosecond Laser and a Phase Mask," *Sensors* **20**(24), 7004 (2020).
14. C. Liao, Y. Wang, D. N. Wang, and L. Jin, "Femtosecond laser inscribed long-period gratings in all-solid photonic bandgap fibers," *IEEE Photonics Technol. Lett.* **22**(6), 425–427 (2010).
15. S. Liu, L. Jin, W. Jin, D. Wang, C. Liao, and Y. Wang, "Structural long period gratings made by drilling micro-holes in photonic crystal fibers with a femtosecond infrared laser," *Opt. Express* **18**(6), 5496 (2010).
16. Y. Kondo, K. Nouchi, T. Mitsuyu, M. Watanabe, P. G. Kazansky, and K. Hirao, "Fabrication of long-period fiber gratings by focused irradiation of infrared femtosecond laser pulses," *Opt. Lett.* **24**(10), 646 (1999).
17. Y. Yu, W. Zhou, J. Ma, S. Ruan, Y. Zhang, Q. Huang, and X. Chen, "High-temperature sensor based on 45° tilted fiber end fabricated by femtosecond laser," *IEEE Photonics Technol. Lett.* **28**(6), 653–656 (2016).
18. R. A. Perez-Herrera, P. Roldan-Varona, M. Galarza, S. Sañudo-Lasagabaster, L. Rodríguez-Cobo, J. M. Lopez-Higuera, and M. Lopez-Amo, "Hybrid Raman-erbium random fiber laser with a half open cavity assisted by artificially controlled backscattering fiber reflectors," *Sci. Rep.* **11**(1), 9169 (2021).
19. R. A. Perez-Herrera, P. Roldan-Varona, L. Rodríguez-Cobo, J. M. Lopez-Higuera, and M. Lopez-Amo, "Single Longitudinal Mode Lasers by Using Artificially Controlled Backscattering Erbium Doped Fibers," *IEEE Access* **9**, 27428–27433 (2021).
20. D. Pallarés-Aldeiturriaga, P. Roldán-Varona, L. Rodríguez-Cobo, and J. M. López-Higuera, "Optical Fiber Sensors by Direct Laser Processing: A Review," *Sensors* **20**(23), 6971 (2020).
21. R. A. Perez-Herrera, M. Bravo, P. Roldan-Varona, D. Leandro, L. Rodríguez-Cobo, J. M. Lopez-Higuera, and M. Lopez-Amo, "Microdrilled tapers to enhance optical fiber lasers for sensing," *Sci. Rep.* **11**(1), 20408 (2021).
22. M.I. Skvortsov, A.A. Wolf, A.V. Dostovalov, O.N. Egorova, S.L. Semjonov, and S.A. Babin, "Narrow-Linewidth Er-Doped Fiber Lasers with Random Distributed Feedback Provided by Artificial Rayleigh Scattering," *J. Light. Technol.* **40**(6), 1829–1835 (2022).
23. P. Roldan-Varona, M. Lomer, J. F. Algorri, L. Rodríguez-Cobo, and J. M. Lopez-Higuera, "Enhanced refractometer for aqueous solutions based on perfluorinated polymer optical fibres," *Opt. Express* **30**(2), 1397 (2022).
24. R.A. Perez-Herrera, A. Stancalie, P. Cabezudo, D. Sporea, D. Neşuş, and M. Lopez-Amo, "Gamma radiation-induced effects over an optical fiber laser: Towards new sensing applications," *Sensors* **20**(11), 3017 (2020).
25. R. A. Perez-Herrera, D. Pallares-Aldeiturriaga, A. Judez, L. Rodríguez-Cobo, M. Lopez-Amo, and J. M. Lopez-Higuera, "Optical fiber lasers assisted by microdrilled optical fiber tapers," *Opt. Lett.* **44**(11), 2669–2672 (2019).
26. W. He, J. Zhao, M. Dong, F. Meng, and L. Zhu, "Wavelength-switchable erbium-doped fiber laser incorporating fiber Bragg grating array fabricated by infrared femtosecond laser inscription," *Opt. Laser Technol.* **127**, 106026 (2020).
27. S. Pevec and D. Donlagić, "Multiparameter fiber-optic sensors: a review," *Opt. Eng.* **58**(07), 1 (2019).
28. X. Wang, D. Chen, H. Li, L. She, and Q. Wu, "Random fiber laser based on artificially controlled backscattering fibers," *Appl. Opt.* **57**(2), 258–262 (2018).